Frontiers in Computing and Intelligent Systems
ISSN: 2832-6024 | Vol. 10, No. 2, 2024

Research on CT System Image based on Back Projection Reconstruction Model

Ruofeng Yu [1,*], Yating Wu [2], Ruoyu Yu [3]

[1] School of Chinese-Western Medicine, Fujian University of Traditional Chinese Medicine Fuzhou Fujian, China
[2] School of Humanities and Management, Fujian University of Traditional Chinese Medicine Fuzhou Fujian, China
[3] School of Law, Xiamen University Tan Kah Kee College Zhangzhou Fujian, China

[*] **Corresponding author**: Ruofeng Yu (Email: 2876283680@qq.com)

Abstract: CT technology has been widely used in clinical medicine, industrial engineering and other fields in contemporary society. Since the traditional back projection reconstruction algorithm will introduce star artifacts, we decide to use a parallel beam filtered back projection reconstruction model based on Radon changes and R-L filters. Since the rotation center of the system does not coincide with the geometric center, the data will be missing when using Radon transformation, so we carry out "edging" processing on the square tray. After processing the data to remove the gain (where the gain coefficient is 2.0033) and removing the "edge" at the end of the filtering, we reconstructed the detected object and obtained the absorption rates of the ten points required by the problem as follows :0.0126, 2.2902, 5.9159, 0.0163, 0.0823, 3.1336, 6.0333, 0.0000, 7.7184, 0.0861.

Keywords: CT System; Parallel Beam Filtering; Edging Treatment; Back Projection Reconstruction.

1. Introduction

Computed Tomography (CT) can make use of the absorption characteristics of radiation energy in samples of biological tissues and engineering materials without destroying the samples, so as to obtain the internal structure information of the samples. A typical two-dimensional CT system is shown in Figure 1, where the parallelly incident X-rays are perpendicular to the detector plane, and each detector unit is regarded as a receiving point and arranged equidistant. The X-ray emitter and detector are fixed relative to each other, and the whole transmitting and receiving system is rotated 180 times counterclockwise around a fixed rotation center. For each X-ray direction, a detector with 512 equidistant elements is used to measure the absorption and attenuation of the two-dimensional media, and 180 groups of received information are obtained after the gain processing.

There are often errors in the installation of CT systems, which will affect the imaging quality, so it is necessary to calibrate the parameters of the installed CT system, that is, to calibrate the parameters of the CT system with the help of samples with known structures (called templates), and image the samples with unknown structures accordingly.

2. Data Source

The data are primarily derived from the experimental results of multiple computed tomography (CT) systems and related data sources on the Internet.

3. Model Establishment and Solution

3.1. The Reconstruction Model of Parallel Beam Filter Backprojection is Established

In this paper, geometric relations and mathematical principles have been employed to calculate a number of parameters pertaining to the CT machine [1], including the position of the rotation centre, the spacing of the detector units and the number of X-ray directions utilised by the instrument. The objective is to optimise the data in order to achieve calibration of the CT machine's parameters.

In order to obtain accurate images and successfully achieve two-dimensional parallel wave back projection reconstruction, it is necessary to establish a parallel beam back projection reconstruction model [2]. The traditional model is a back projection reconstruction model [3], but it has a significant drawback in that it will introduce star artefacts[4]. Therefore, it is essential to introduce a filter function and construct a parallel beam filter back projection model. The modelling process is divided into two parts: in the first part, the data is transformed by Radon based on the absorption rate [5], and in the second part, an RL filter is employed for filtering[6].

3.1.1. Radon Transformation and its Properties

Let us consider the function f(x,y) to be the density function of the object to be reconstructed. Its Radon transform is defined as the integral of a curve of the first kind along a set of parallel X-rays:

$$R(\varphi, r) = \int_{L(\theta,r)} f(x,y)ds \quad (1)$$

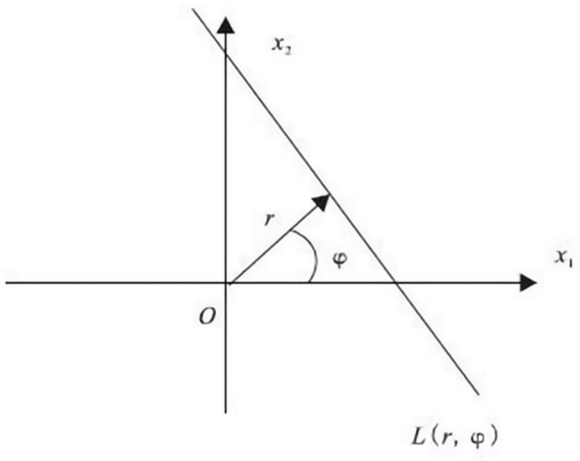

Figure 1. Google Scholar

In this context, $R(\varphi, r)$ represents the Radon transform of

the function $f(x,y)$. Each ray M is defined by two parameters: θ and r. The first of these, φ, denotes the angle between the vertical line of ray M and the X-axis, while r denotes the distance from the origin of ray L (see Figure 1).

The complete set of one-dimensional projections of $f(x,y)$ is provided for each two-dimensional image object. By employing the variable $r = x\cos\varphi + y\sin\varphi$ and the sampling characteristics of the impulse function, we can derive the following:

$$R(\varphi, r) = \iint_{(L^2)} f(x,y)\delta(x\cos\varphi + y\sin\varphi - y)dxdy \quad (2)$$

The aforementioned description provides an account of the definition of the Radon transform.

The object to be scanned is reproduced in exact scale, eliminating the necessity for consideration of isotropic scaling, rotation, or translation of the function $f(x,y)$.

Let us consider the parallel beam projection of $f(x,y)$ at angles $\varphi - \varphi_0$, which we shall denote by $p_\varphi(X_r)$. Theoretically, the projection $p(x)$ and the density distribution function $f(x,y)$ can be expressed as the accumulation of one-dimensional line integrals in the time domain. However, it is challenging to identify a method of projection reconstruction based on line integrals. The Fourier slice theorem offers a more straightforward mathematical relationship between projection and image in the frequency domain. Its mathematical expression is as follows:

$$F_1\left[p_\varphi(X_r)\right] = F(p,\varphi)|_{\varphi=\varphi_0} \quad (3)$$

The problem of projection image reconstruction can be solved according to the following process: firstly, the projection must be collected under different angles. Secondly, the one-dimensional Fourier transform of each projection must be found. Thirdly, the two-dimensional Fourier transform of the image must be obtained by applying the Fourier theorem. Fourthly, the slices of the two-dimensional Fourier transform of the image must be gathered into the 2D Fourier transform of the image. Finally, the reconstructed image must be obtained by inverse transformation.

3.1.2. R-L Filter

In accordance with the aforementioned principles, we have elected to adopt the R-L filter. The discrete form of the R-L filter was initially proposed by Indian scholars Ramachandran and Lakshminarayanan, whose frequency domain number is[7]:

$$H_{R-L}(p) = |p|W(p) = |p|rect\left(\frac{p}{2B}\right) \quad (4)$$

Formula:

$$rect\left(\frac{p}{2B}\right) = \begin{cases} 1, |p| < B = \frac{1}{2d} \\ 0, other \end{cases} \quad (5)$$

In this context, p represents the spatial frequency, while $W(p)$ denotes the window function.

The corresponding time-domain convolution function, $h_{R-L}(X_r)$, is given by:

$$h_{R-L}(X_r) = 2B^2\sin c(2x,B) - B^2\sin c^2(x,B) \quad (6)$$

The discrete form of $h_{R-L}(X_r)$ is derived by substituting $x_r = nd$ into equation (6).

$$h_{R-L}(X_r) = \begin{cases} \frac{1}{4d^2} & ,n = 0 \\ 0 & ,n = Even\ number \\ \frac{-1}{n^2\pi^2d^2} & ,n = Odd\ number \end{cases} \quad (7)$$

R-L filter form is simple and practical, the reconstruction effect is good, the outline is clear.

3.1.3. Parallel Beam Filter Back Projection Reconstruction Model

Let the image to be reconstructed be $b(x,y)$and its two-dimensional Fourier transform be $B(w_1,w_2)$. According to the Fourier slice theorem,$\hat{B}(p,\theta)$ can be obtained by the one-dimensional Fourier transform of the projection $p_\varphi(X_r)$ of $b(x,y)$ under different angles φ, i.e. :

$$B(w_1,w_2) = \hat{B}(p,\theta) = F_1\left[p_\varphi(X_r)\right] = P(p,\varphi) \quad (8)$$

It is necessary to reconstruct the image.

$$\hat{b}(p,\theta) = b(x,y) = F_2^{-1}[B(w_1,w_2)] = \int_0^\pi d\varphi \int_{-\infty}^{\infty} |p|P(p,\varphi)e^{j2\pi pr\cos(\theta-\varphi)} \quad (9)$$

The integral of the second half of the above equation is written as the inverse Fourier transform of the spatial variable ($X_r = r\cos(\theta-\varphi)$):

$$\begin{aligned}\int_{-\infty}^{\infty} |p|P(p,\varphi)e^{j2\pi pr\cos(\theta-\varphi)}dp &= \int_{-\infty}^{\infty} |p|P(p,\varphi)e^{j2\pi prX_r}dp \\ &= h(X_r) * p(X_r,\varphi) \\ &= g(X_r,\varphi) \\ &= g(r\cos(\theta-\varphi),\varphi) \quad (10)\end{aligned}$$

Formula:

$$g(X_r,\varphi) = h(X_r) * p(X_r,\varphi) \quad (11)$$

It can be demonstrated that

$$\hat{b}(r,\theta) = \int_0^\pi g[r\cos(\theta-\varphi)]d\varphi \quad (12)$$

The physical meaning of the above formula is as follows: the cumulative back projection reconstruction of all the filtered ray projections at a given point (r,θ) in the range of $0\sim\pi$ is obtained, and the pixel value of the point (r,θ) is obtained. This is the filtered back projection equation [8], which can concentrate the various steps of the filtered back projection algorithm.

In summary, we will use parallel beam filter back projection to reconstruct the model and solve the model.

3.2. Realization and Problem Solving of the Reconstructed Model of Parallel Beam Filter Backprojection

In accordance with the aforementioned algorithmic principle, the iradon function within the MATLAB software program represents a filter backprojection function based on the R-L filter. Consequently, this model can be directly implemented through the iradon function.

3.2.1. Scale Factor Processing

Given that the data has undergone gain processing, it is essential to ascertain the relationship between the data obtained by the computer and the data after gain processing when utilising the computer for back projection. In this regard, a back-projection calculation was initially performed on the data, the absorptivity of each pixel was obtained, and a relationship function was established between the two. The absorptivity obtained by the computer was then found to be approximately proportional to the original absorptivity [9] of the data, with a proportional coefficient of k=2.033, as determined by MATLAB.

$$X_2 = kX_1 \quad (13)$$

In this context, X_1 represents the absorption rate calculated by the computer, while X_2 denotes the original absorption rate.

3.2.2. "Edging" Treatment

As a consequence of the installation error, the centre of rotation is not aligned with the geometric centre of the square tray. This results in a significant discrepancy when utilising the iradon function directly. In light of the aforementioned

considerations, the "edging" treatment was applied to the square tray (as illustrated in Figure 2). This procedure entailed the transformation of the geometric centre of the square tray, designated as "○", to the rotation centre, represented by "×". Consequently, the geometric centre of the resulting edged square, indicated as "×", became the rotation centre[10].

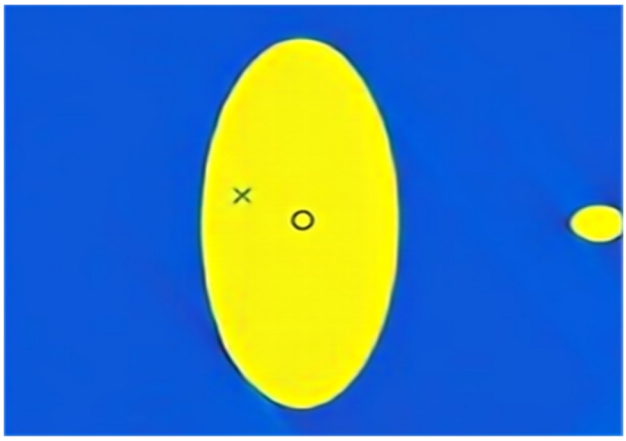

Figure 2. Geometric relationship diagram of large square and component after edging treatment

Following the application of the 'edging' treatment to the square tray, the resulting 'new large square tray' exhibits a rotation centre situated at the tray's centre point, thereby eliminating the system error. At this juncture, the iradon function can be employed directly to calculate the filtered back projection.

3.2.3. Filter Back Projection Calculation

The corresponding program was developed using MATLAB software, and the filtered back projection of the data was calculated using the iradon function. The resulting calculations are presented in Figure 3.

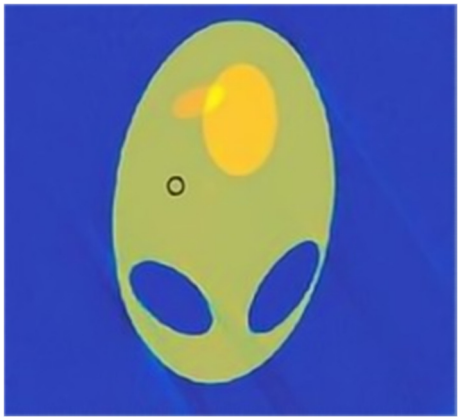

Figure 3. Inversion reconstruction after "edging"

In order to obtain the geometry of the object to be scanned on the actual square tray and its determined position, it is also necessary to carry out the process of "edge removal". The resulting operation, following the completion of the aforementioned edge removal and the multiplication by the scale coefficient, is illustrated in Figure 4.

Figure 4. Inversion map after removing the "edging"

The ten determined points are presented in Table 1, which also shows the parameters of each point:

Table 1. Ten determined point absorptivity

X	Y	Absorptivity
10.0000	18.0000	0.0000
34.5000	25.0000	0.9722
43.5000	33.0000	0.0036
45.0000	75.5000	1.1761
48.5000	55.5000	1.0426
50.0000	75.5000	1.4652
56.0000	76.5000	1.2849
65.5000	37.0000	0.0007
79.5000	18.0000	0.0000
98.5000	43.5000	0.0175

Subsequently, the Wiener2 filter is employed for the purpose of noise reduction and colour level processing, thereby facilitating the generation of the image, as illustrated in Figure 5.

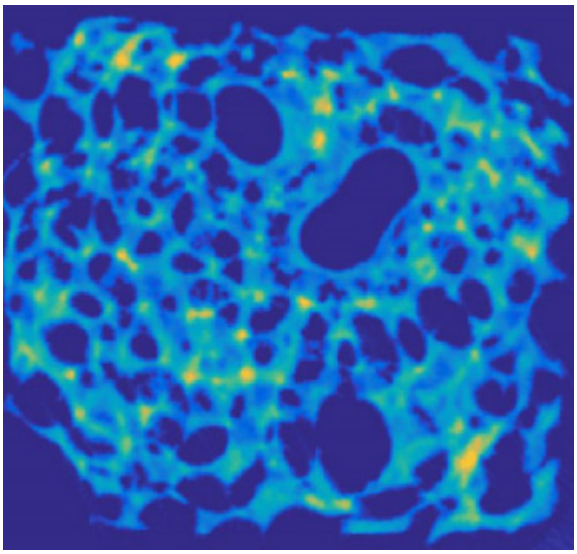

Figure 5. Reconstructed image after noise reduction

The ten determined points are presented in Table 2, which also shows the parameters of each point:

Table 2. Absorption rate after noise reduction at ten definite points

X	Y	Absorptivity
10.0000	**18.0000**	**0.0126**
34.5000	**25.0000**	**2.2902**
43.5000	**33.0000**	**5.9159**
45.0000	**75.5000**	**0.0163**
48.5000	**55.5000**	**0.0823**
50.0000	**75.5000**	**3.1336**
56.0000	**76.5000**	**6.0333**
65.5000	**37.0000**	**0.0000**
79.5000	**18.0000**	**7.7184**
98.5000	**43.5000**	**0.0861**

4. Conclusion

The models established by us can solve the problems of parameter calibration and image reconstruction well, and the scope of application is easy to popularize. Different filtering functions can be adopted for different problems to eliminate the influence of different factors on the absorption rate.

5. Literature References

References must be cited in the text within brackets in numerical order, starting with [1]. Do not use Word's automated numbering features. Consecutive reference number citations should be indicated with an n-dash (–) [2–4] or a comma [5, 6] as necessary. In sentences, use the author names instead of "Reference [7]" or "as in [8]" (e.g., "Smith and Smith [9] show ...").

The reference list must be typed in manually. Do not use Word's References feature or numbered list. In the reference list, provide up to three authors' names; if more than three authors, use "et al." Place a space between an authors' initials. Papers that have not been published should be cited as "unpublished" [7]. Papers that have been submitted or accepted for publication should be cited as "submitted for publication" [8]. Please give affiliations and addresses for personal communications [9]. Use sentence case for the words in a paper title.

6. Conclusion

The manuscript should include a conclusion. In this section, summarize what was described in your paper. Future directions may also be included in this section. Authors are strongly encouraged not to reference multiple figures or tables in the conclusion; these should be referenced in the body of the paper.

References

[1] Ali E M A ,Strubel N ,Pinkney L , et al.Pediatric contrast-enhanced chest CT on a photon-counting detector CT: radiation dose and image quality compared to energy-integrated detector CT[J].Pediatric Radiology,2024,(prepublish):1-12.

[2] Zoubeida M ,Nabil C ,Amina S , et al.A Quantitative Comparative Study of Back Projection, Filtered Back Projection, Gradient and Bayesian Reconstruction Algorithms in Computed Tomography (CT)[J].International Journal of Probability and Statistics,2015,4(1):20.

[3] Shu Z ,Entezari A .RBP-DIP: Residual back projection with deep image prior for ill-posed CT reconstruction[J].Neural Networks,2024,180106740-106740.

[4] Taylor B ,Elliott B ,Conneller C , et al.Resolving the Issue of Artefact Deposition at Star Carr[J].Proceedings of the Prehistoric Society,2017,8323-42.

[5] Hung Y K J ,Arndt A K ,Murphy P , et al.Slow post-fire carbon balance recovery despite increased net uptake rates in Alaskan tundra[J].Environmental Research Letters,2024, 19(12): 1240 13-124013.

[6] Luo Z ,Ma H ,Shi D , et al.GFANC-RL: Reinforcement Learning-based Generative Fixed-filter Active Noise Control. [J]. Neural networks : the official journal of the International Neural Network Society,2024,180106687.

[7] Michele G D ,Luigi L ,Cristoforo M , et al.Signal-to-Noise Ratio Analysis for the Voltage-Mode Read-Out of Quartz Tuning Forks in QEPAS Applications [J]. Micromachines, 2023, 14(3):619-619.

[8] Jafari S ,Kolivand S .Performance of Iterative Reconstruction in Image Space Algorithm in Combination with Automatic Tube Current Modulation Compared to Filtered Back Projection in Brain CT Scan.[J].Journal of biomedical physics & engineering,2024,14(4):379-388.

[9] Guk I ,Shandybina G ,Yakovlev E .Influence of accumulation effects on heating of silicon surface by femtosecond laser pulses[J].Applied Surface Science,2015,353851-855.

[10] Du Y ,Liu Y ,Wu H , et al.Combination of edge enhancement and cold diffusion model for low dose CT image denoising. [J]. Biomedizinische Technik. Biomedical engineering,2024.